

## Supporting Information

### Photothermal Slippery Surface towards Spatial Droplets Manipulation

Keyu Han,<sup>a</sup> Zubin Wang,<sup>b</sup> Liping Heng\*<sup>a</sup> and Lei Jiang<sup>a</sup>

<sup>a</sup> School of Chemistry, Beihang University, Beijing 100191, China. E-mail: henglp@buaa.edu.cn;

Fax: +86 10-82627566.

<sup>b</sup> School of Materials Science and Engineering, Zhengzhou University, Zhengzhou 450052, P. R.

China.

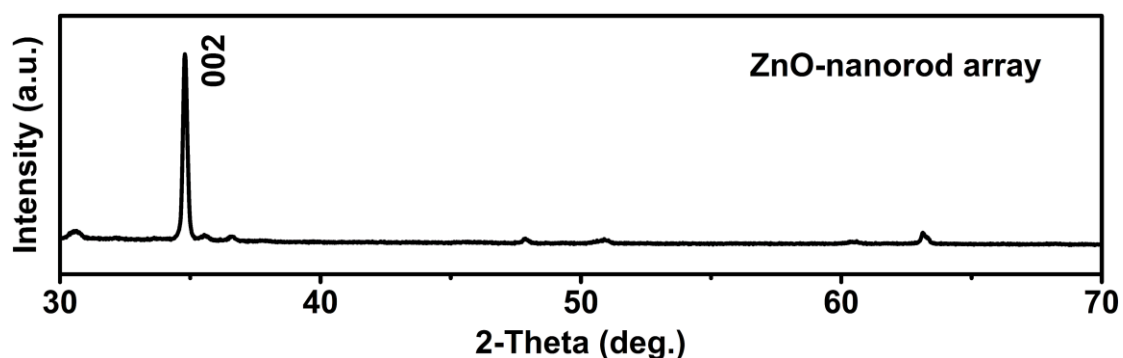


**Fig. S1** X-ray diffraction (XRD) pattern of ZnO-nanorod array grown on indium tin oxide (ITO) glass substrate with a remarkable (002) peak, which clearly indicate that ZnO (001) planes are oriented parallel to the basal plane of ITO and the ZnO nanorods were perpendicularly aligned onto the substrate.

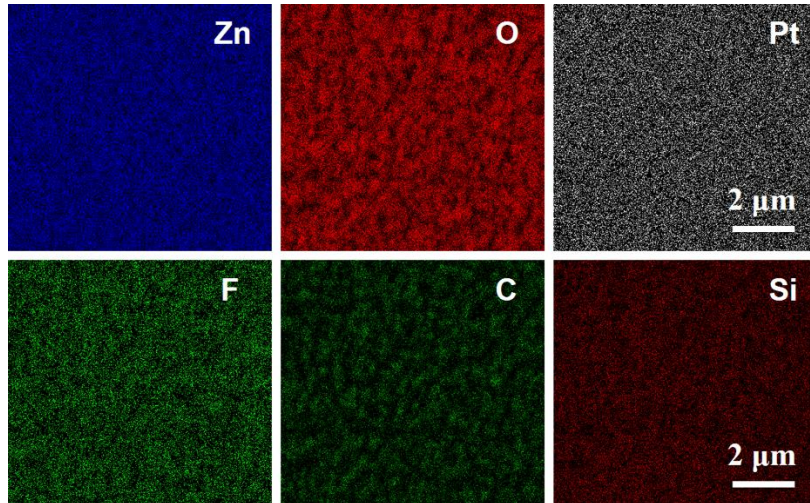


**Fig. S2** SEM EDS element mapping images of ZnO-FAS-Pt surface, suggestive of successful Pt deposition and FAS modification on the ZnO surface.

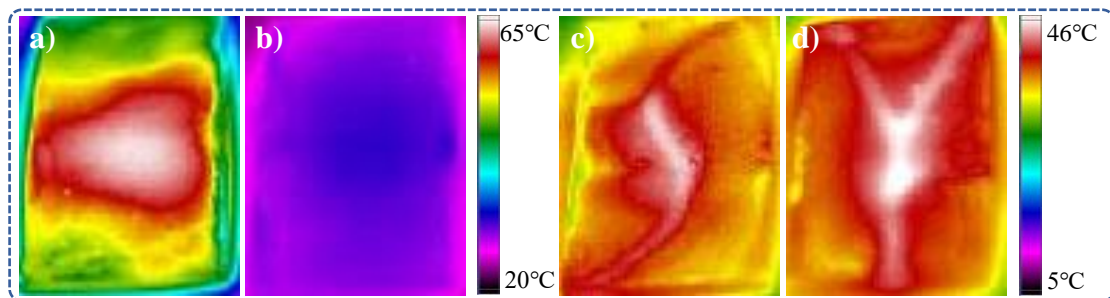


**Fig. S3** Recorded infrared images of the various surfaces. The infrared images of the (a) ZFPFSS and (b) ZnO-paraffin surface after illumination for 120 s. The infrared images of the ZFPFSS with different droplet-guiding pathways (c) 'S' type and (d) 'Y' type.

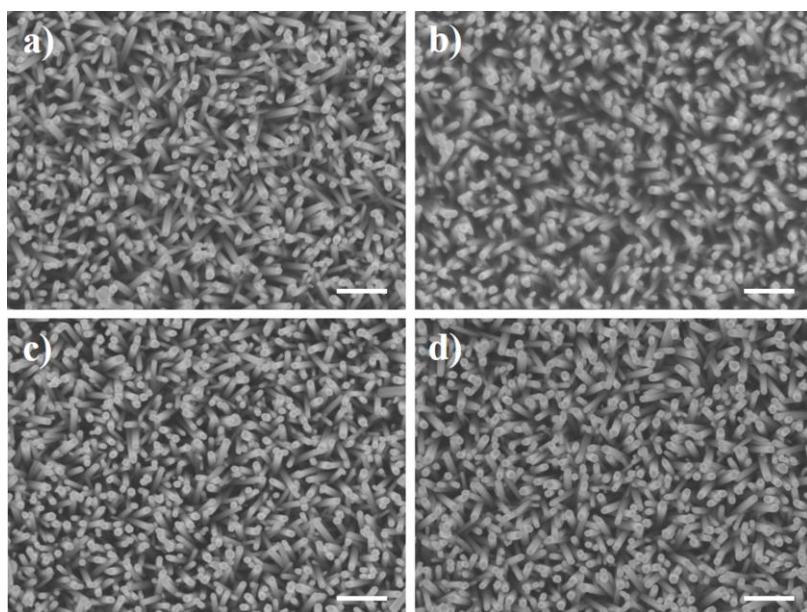


**Fig. S4** Top-view SEM images of the as-prepared Pt-coated ZnO-nanorod array with different Pt deposition time. a) 120 s, b) 240 s, c) 360 s and d) 480 s. The results show that Pt deposition can gradually increase the diameters of the ZnO nanorods. Specifically, the average diameters of the nanorods are  $58.1 \pm 3.7$ ,  $60.2 \pm 5.9$ ,  $62.8 \pm 4.4$  and  $66.7 \pm 4.5$  nm for Pt deposition times of 120, 240, 360, and 480 s, respectively. The scale bar is 500 nm.

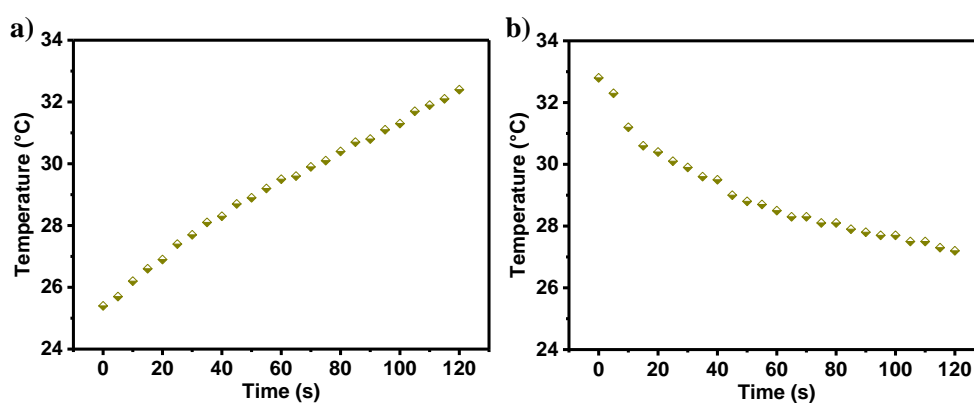


**Fig. S5** The temperature change processes of the ZnO-paraffin under 3 sun light illumination (a) turning on the light (melting process) and (b) turning off the light (solidification process).

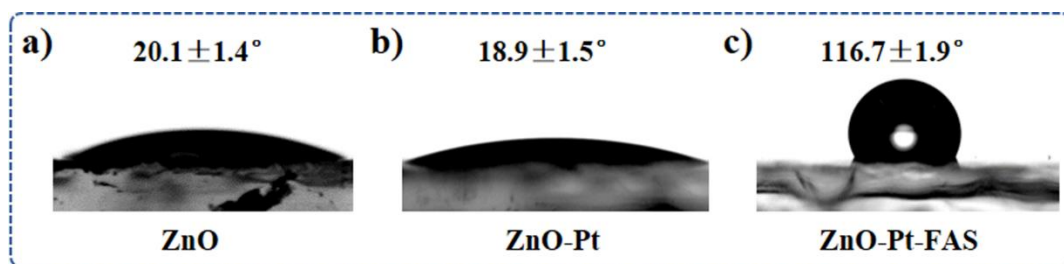


**Fig. S6** Water CAs of the (a) ZnO film (b) the ZnO-Pt film and (c) the ZnO-Pt film modified with FAS, respectively.

**Table S1** The surface tensions of the test liquids used in the work.

| Liquid                                | water | glycerol | formamide | ethylene glycol | dimethyl phthalate | ionic liquid |
|---------------------------------------|-------|----------|-----------|-----------------|--------------------|--------------|
| Surface tension (mN m <sup>-1</sup> ) | 72.1  | 62.7     | 57.4      | 47.7            | 42.6               | 31.3         |

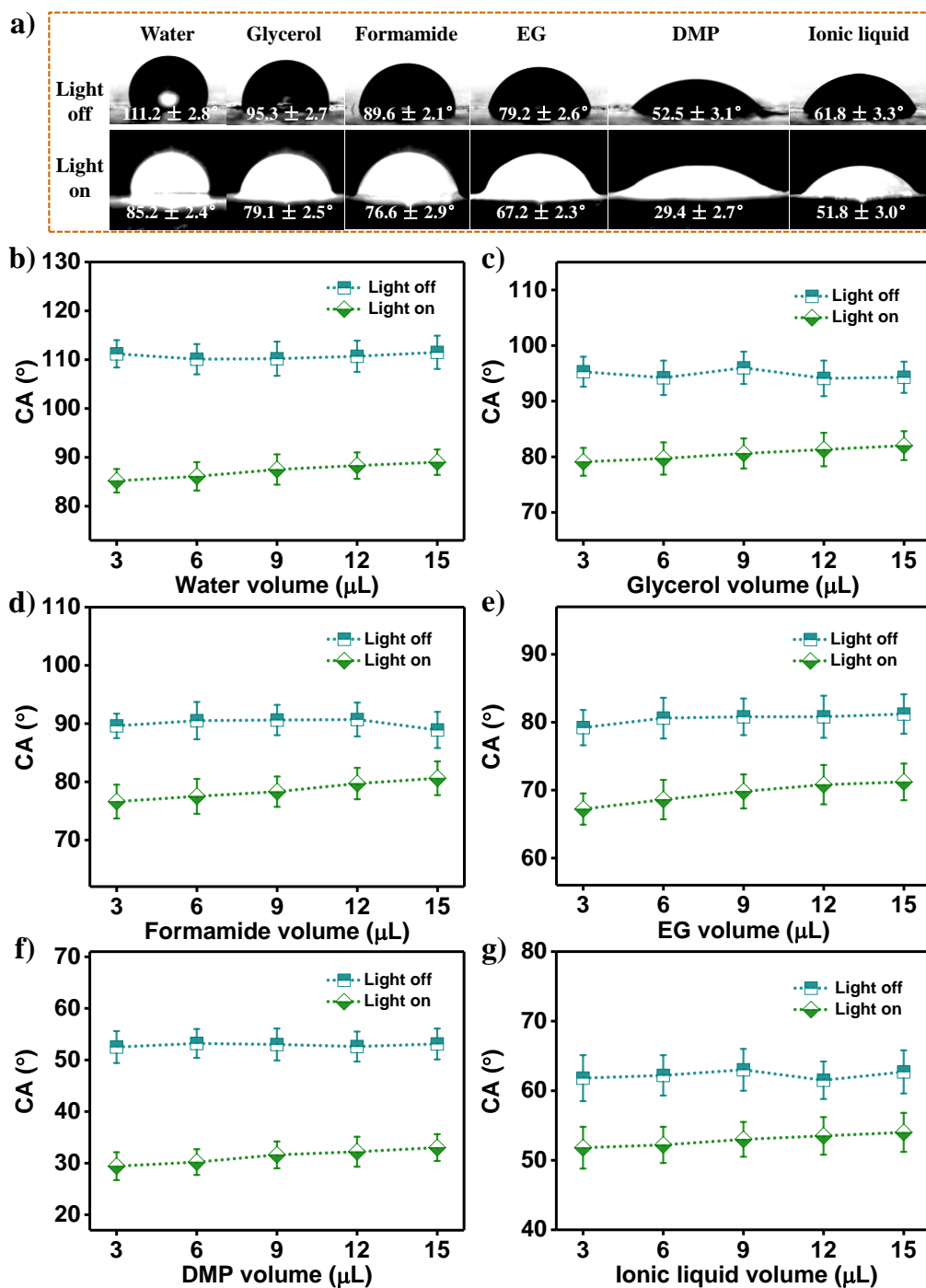


**Fig. S7** (a) CA photos of various liquid droplets (3  $\mu\text{L}$ ) on ZPFSS with light off and on. CAs of (b) water, (c) glycerol, d) formamide, e) ethylene glycol (EG), (f) dimethyl phthalate (DMP), (g) ionic liquid with various volumes on the ZPFSS with light off and on.

### The long-term stability of the ZFPFSS

After storage at ambient condition for 180 d without diaphragmation, the droplet SAs on the ZFPFSS were recorded without light and under light illumination. As shown in Figure S8, after storage for 180 d, the ZFPFSS showed SAs of  $90^\circ$ ,  $63.5 \pm 2.9^\circ$ ,  $66.4 \pm 3.2^\circ$ ,  $68.9 \pm 3.3^\circ$ ,  $73.6 \pm 2.7^\circ$  and  $74.8 \pm 3.0^\circ$  for water, glycerol, formamide, EG, DMP and ionic liquid droplets without illumination, respectively, which were no obvious change in comparison with those on the pristine ZFPFSS (Figure 3a). Under light irradiation, the SAs of water, glycerol, formamide, EG, DMP and ionic liquid droplets decreased to  $8.4 \pm 1.7^\circ$ ,  $8.6 \pm 1.5^\circ$ ,  $9.3 \pm 1.9^\circ$ ,  $7.9 \pm 1.6^\circ$ ,  $9.2 \pm 1.4^\circ$  and  $8.1 \pm 2.0^\circ$ , respectively, which were well agreement with those on the pristine surface (Figure 3a). The small SAs ( $< 10^\circ$ ) suggested that the surface retained the excellent slippery property after storage at ambient condition for 180 d without diaphragmation. Therefore, the ZFPFSS possessed superior long-term stability.

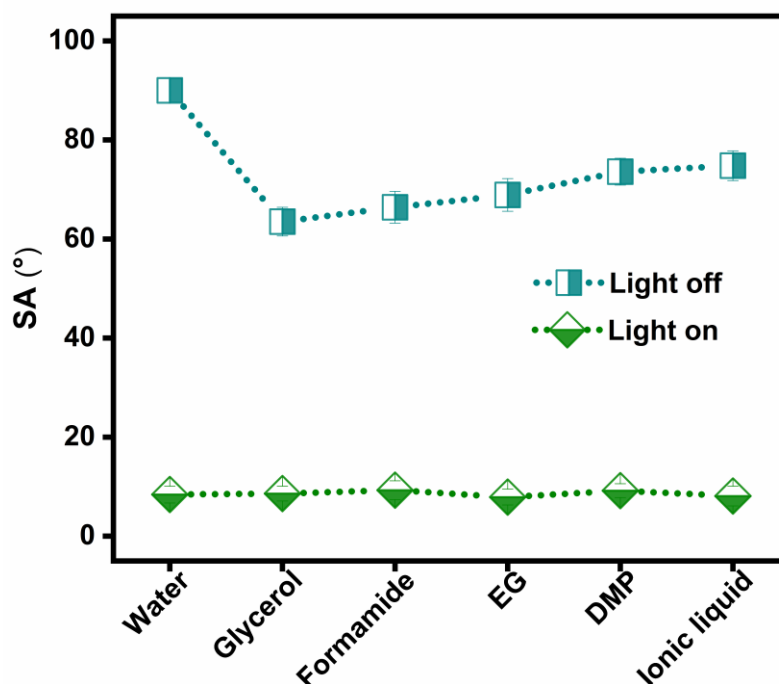


**Fig. S8** The SAs of droplets on the ZFPFSS after storage at ambient conditions for 180 d without diaphragmation, demonstrating excellent long-term stability.

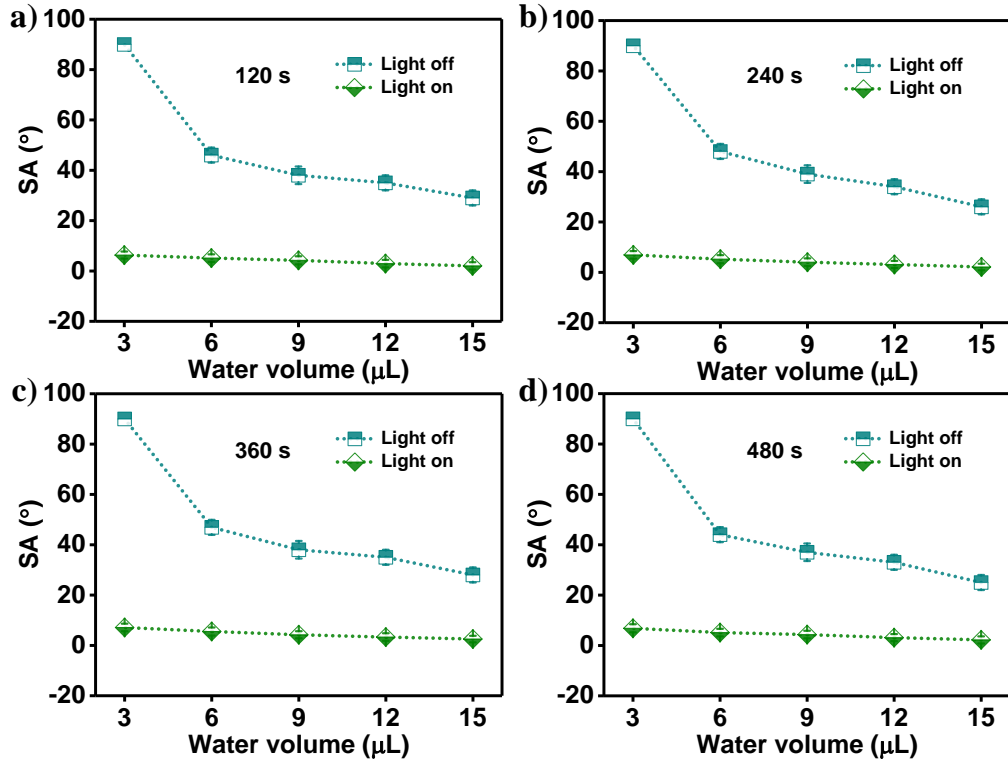


**Fig. S9** SA values of water with various volumes on the ZFPSSs fabricated through different Pt deposition time (a) 120 s, (b) 240 s, (b) 360 s, (b) 480 s without and with light illumination. With the increase of droplet volumes, all the water SAs gradually decreased under light illumination and sharply decreased without light illumination. The water droplets showed almost the same SAs on the above ZFPSSs, showing no effect of Pt sputtering time on the surface slippery property.

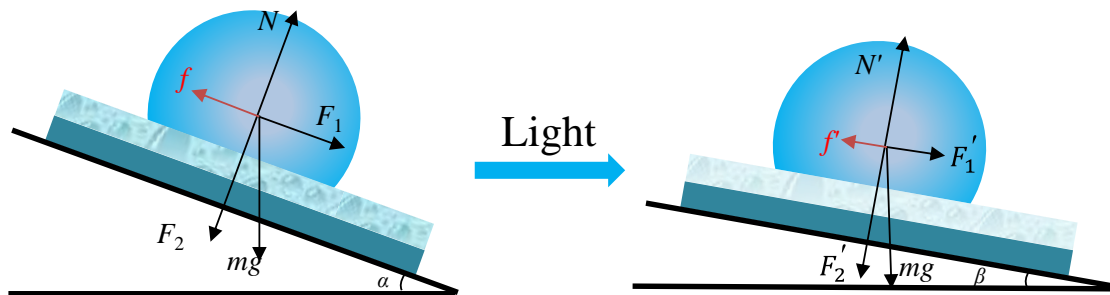


**Fig. S10** Schematic illustration demonstrating the force analysis of liquid droplets on the tilted ZFPSS without and with irradiation.

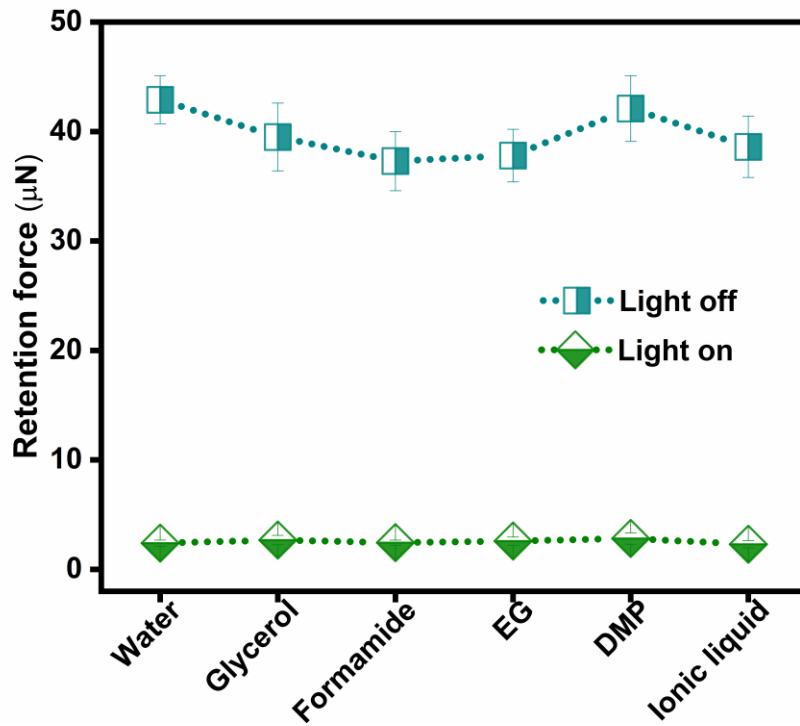


**Fig. S11** The retention forces between the liquid droplets and the surface in the dark and under light illumination.

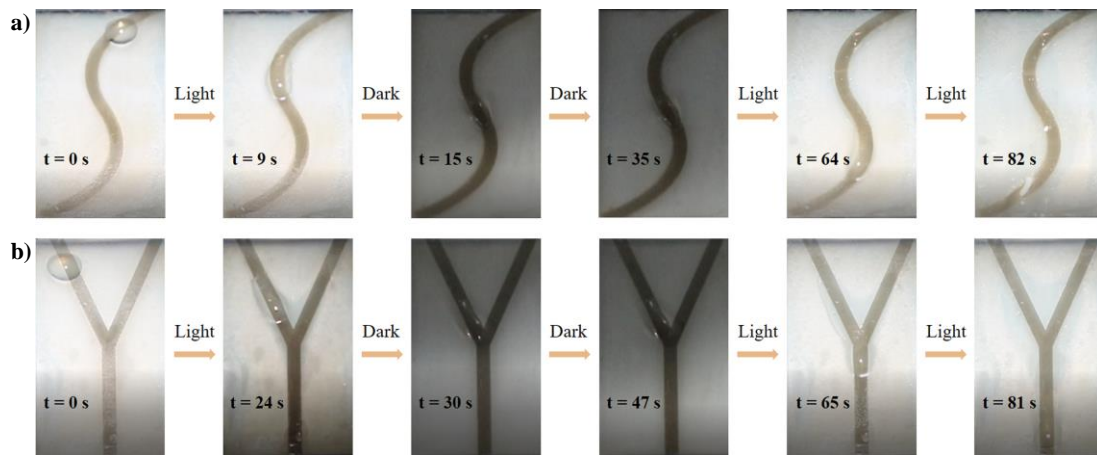


**Fig. S12** The light manipulation of DMP droplets on the ZFPFSS with S-shape and Y-shape pathways.

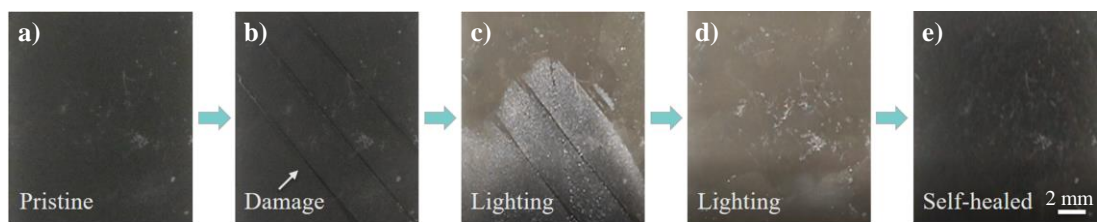


**Fig. S13** The photothermal self-healing process of the ZFPFSS.

**Movie S1.** The glycerol droplet sliding on the ZFPFSS with S-shape pathway under light illumination.

**Movie S2.** The glycerol droplet sliding on the ZFPFSS with Y-shape pathway under light illumination.